Enhancement in energy storage performance of the P(VDF-HFP)-based composites by adding PLZST inorganic nanoparticles

Yan Guo,[a] Di Zhou,[*a] Ran Xu,[a] Qingshan Zhu,[a] Da Li,[a] WeiChen Zhao,[a] LiXia Pang,[b] Yifei Wang,[c] Wenfeng Liu,[d] Jinzhan Su,[e] Tao Zhou,[f] and Shikuan Sun[g]

[a] Electronic Materials Research Laboratory & Multifunctional Materials and Structures, Key Laboratory of the Ministry of Education & International Center for Dielectric Research, School of Electronic Science and Engineering, Xi'an Jiaotong University, Xi'an, Shaanxi 710049, China.

[b] Micro-optoelectronic Systems Laboratories, Xi'an Technological University, Xi'an, Shaanxi, 710032, China.

[c] Electrical Insulation Research Center, Institute of Materials Science, University of Connecticut, 97 North Eagleville Road, Storrs, CT 06269, USA.

[d] State Key Laboratory of Electrical Insulation and Power Equipment, Xi'an Jiaotong University, Xi'an 710049, Shaanxi, China.

[e] International Research Centre for Renewable Energy, State Key Laboratory of Multiphase Flow in Power Engineering, Xi'an Jiaotong University, Xi'an, Shaanxi, 710049, China.

[f] School of Electronic and Information Engineering, Hangzhou Dianzi University, Hangzhou 310018, China.

[g] School of Material Science and Energy Engineering, Foshan University, Foshan, Guangdong, 528000, P. R. China (38466053@qq.com).

[*]Corresponding author E-mail address: zhoudi1220@gmail.com (Di Zhou)

Finite element simulation:

The electric field distribution in the PLZST/PVDF composite was analyzed by COMSOL electrostatics module. Two-dimensional models with a dimension of 10 ×20 μm2 were established, where triangle mesh was applied to simulation. The dielectric constants of PLZST and PVDF were set as 550 and 8.6 respectively. A high voltage of 5 kV was applied as the top boundary condition, while the bottom boundary was grounded. The composites with different contents of PLZST were simulated for comparison.

The growth process of electrical trees in the PLZST/P(VDF-HFP) nanocomposites was simulated using COMSOL electrostatics module. In the simulation system, a rectangular lattice with a size of 8 × 10 μm^2 is designed. The terminal voltage is set as 4800 V at room tempeauture. The permittivities of the PLZST and P(VDF-HFP) were set as 550 and 8.6, respectively. In the dielectric breakdown model (DBM), the probability of tree channel growth is shown in the following formula:

$$P\left(i,k\rightarrow i^{'},k^{'}\right)=A\frac{\left(\Phi_{i^{'}k^{'}}\right)^{\eta}}{\sum\left(\Phi_{i^{'}k^{'}}\right)^{\eta}}+B\frac{\Phi_{i^{'}k^{'}}}{\Phi_0}+c$$

Φ_0 is a threshold of electric potential, and the fractal dimension η = 3. The coefficients of A, B, and C decide the weight of each term in the equation.

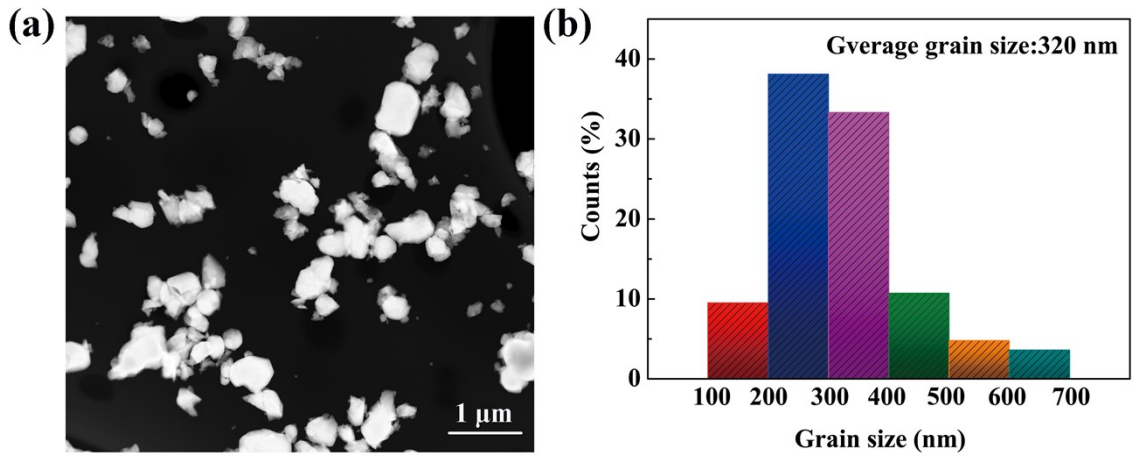

Fig S1. (a) TEM micrographs and (b) grain size distribution of the PLZST NPs.

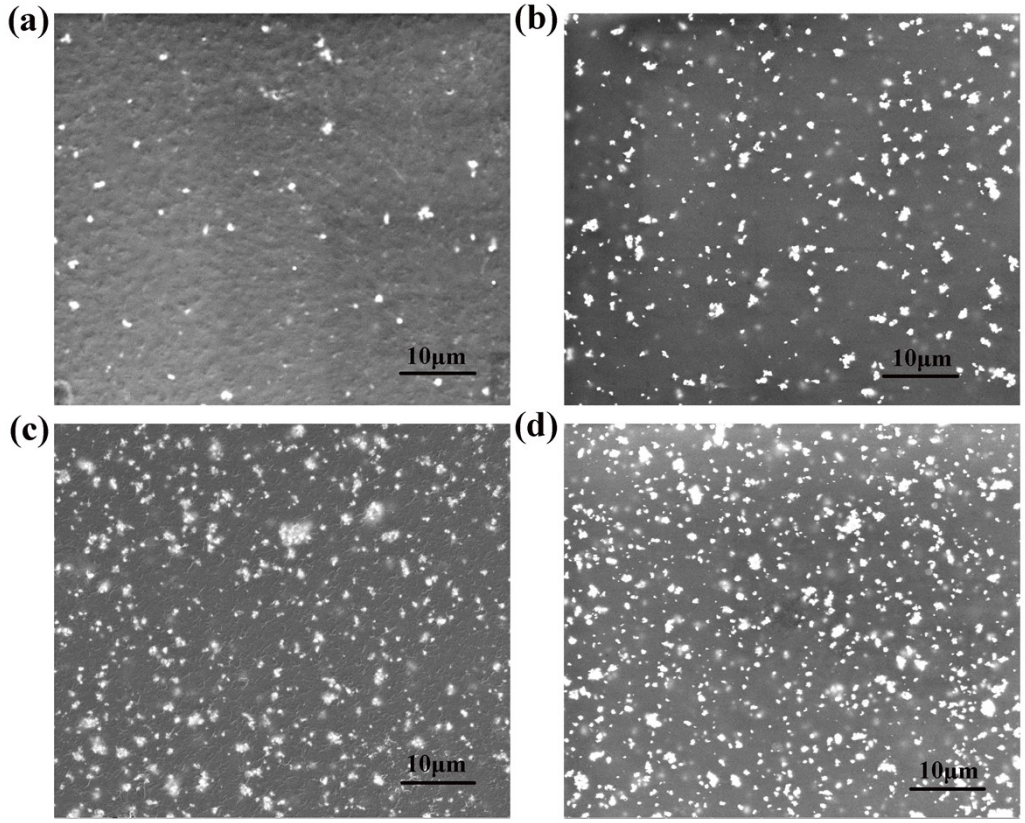

Fig S2. Surface SEM images of PLZST/P(VDF-HFP) nanocomposites. (a) 0.3vol% PLZST; (b) 0.5vol% PLZST; (c) 0.7vol% PLZST; (d) 1.0vol% PLZST.

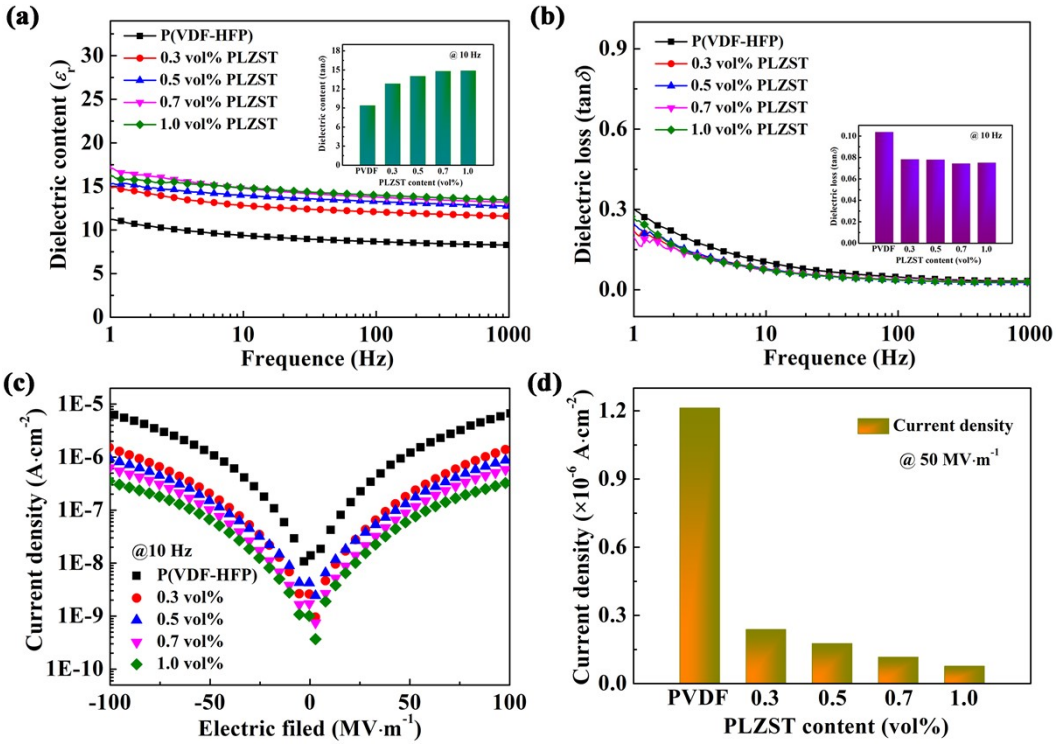

Fig.S3 (a) and (b) The dielectric content and dielectric loss of PLZST/P(VDF-HFP)

nanocomposites at low frequencies. (c) The leakage current density of nanocomposites with different PLZST contents at 10 Hz. (d) At 50 MV·m^{-1}, the leakage current density of PLZST/P(VDF-HFP) nanocomposites.

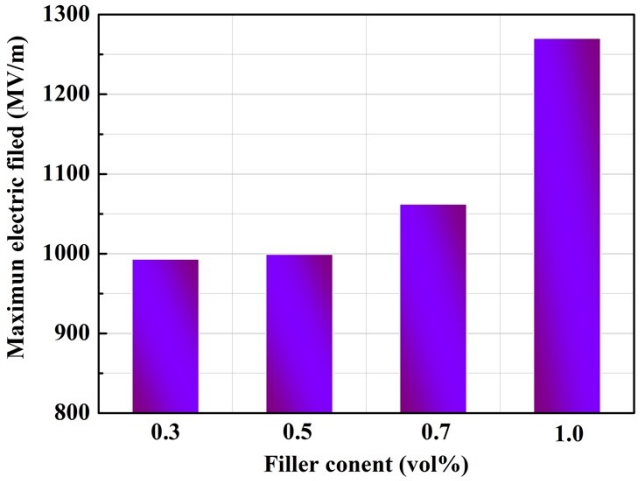

Fig S4. The highest global electric field strength of PLZST/P(VDF-HFP) composites.

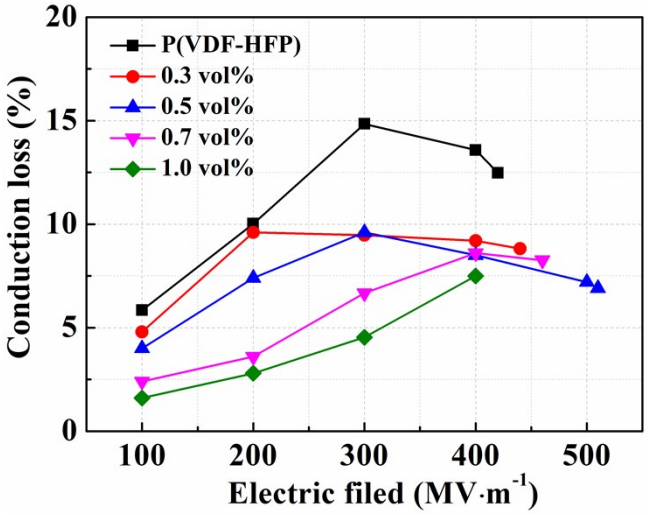

Fig S5. The conduction loss of PLZST/P(VDF-HFP) nanocomposites.

Table S1. Comparison of energy storage properties of PLZST/P(VDF-HFP) nanocomposites with other representative dielectric polymers and nanocomposites.

Samples	E_b (MV/m)	U_e (J/cm^3)	η (%)	Reference
BT/PVDF/PI	370	14.2	51.2	[1]
BT-CF/PVDF	263	5.6	57	[2]
BT-BLN/PVDF	497	14.2	55.5	[3]
BT-Ag/PVDF	350	10.25	64	[4]
BZT-BCT/PVDF	310	7.86	58	[5]
CCTO@Al_2O_3/PVDF	340	8.46	54	[6]
BNNS/BT/PVDF	600	13	71	[7]
BT/PTFMPCS	466	14.64	52.5	[8]
ST@PDA/PVDF	360	9.12	61.1	[9]
BT/PVDF	410	16.2	62	[10]
PDA-SiO_2@BT/PVDF	510	14.7	68	[11]
MXene/PVDF	280	7.8	65	[12]
BT@ Al_2O_3/PVDF	450	12.37	63.7	[13]
NBT/PVDF	350	11.7	63.21	[14]
BT/MgO/PVDF	416	15.55	68	[15]
c-PVDF/BNNS/mBT	400	5.2	68	[16]
BT@TiO_2/PVDF	500	9.95	65	[17]
BZT/PVDF	380	6.3	67.1	[18]
mBT/PVDF	517	11.27	60	[19]
NBT-SBT/PVDF	500	15.3	60	[20]
PLZST/PVDF	510	15.83	74.17	This work

References

1 B. Xie, Q. Zhang, L. Zhang, Y.W. Zhu, X. Guo, P.Y. Fan, and H.B. Zhang, *Nano Energy*, 2018, **54**, 437-446.

2 Q. M. Wang, J. M. Zhang, Z. D. Zhang, Y. N. Hao, and K. Bi, *Adv. Compos. Hybrid*

Mater., 2020, **3**, 58-65.

3 P. J. Wang, D. Zhou, J. Li, L. X. Pang, W. F. Liu, J. Z. Su, C. Singh, S. Trukhanov, and A. Trukhanov, *Nano Energy*, 2020, **78**, 105247.

4 H. C. Liu, S. B. Luo, S. H. Yu, S. J. Ding, Y. B. Shen, R. Sun, and C. P. Wong, *IEEE Trans. Dielectr. Electr. Insul.*, 2017, **24**, 757-763.

5 Q. G. Chi, T. Ma, Y. Zhang, Y. Cui, C. H. Zhang, J. Q. Lin, X. Wang and Q. Q. Lei, *J. Mater. Chem. A*, 2017, **5**,16757.

6 Q. G. Chi, X. B. Wang, C. H. Zhang, Q. G. Chen, M. H. Chen, T. D. Zhang, L. Gao, Y. Zhang, Y. Cui, X. Wang, and Q. Q. Lei, *ACS Sustainable Chem. Eng.*, 2018, **6**, 8641-8649.

7 Y. S. Li, Y. Zhou, S. Cheng, J. Hu, J. L. He and Q. Li, *Mater.*, 2021, **14**, 4780.

8 H. Luo, S. Chen, L. H. Liu, X. F. Zhou, C. Ma, W. W. Liu and D. Zhang, *ACS Sustainable Chem. Eng.*, 2019, **7**, 3145-3153.

9 L. M. Yao, Z. B. Pan, J. W. Zhai, G. Z. Zhang, Z. Y. Liu, and Y. H. Liu, *Compos. Part A*, 2018, **109**, 48-54.

10 Y. F. Wang, J. Cui, L. X. Wang, Q. B. Yuan, Y. J. Niu, J. Chen, Q. Wang and H. Wang, *J. Mater. Chem. A*., 2017, **5**, 4710-4718.

11 M. J. Feng, C. H. Zhang, G. T. Zhou, T. D. Zhang, Y. Feng, Q. G. Chi and Q. Q. Lei, *IEEE Access*, 2020, **8**, 81542-81550.

12 W. Y. Li, Z. Q. Song, J. M. Zhong, J. Qian, Z. Y. Tan, X. Y. Wu, H. Y. Chu, W. Nie, and X. H. Ran, *J. Mater. Chem. C.*, 2019, **7**, 10371.

13 Z. B. Pan, L. M. Yao, J. W. Zhai, K. Yang, B. Shen, and H. T. Wang, *ACS Sustainable Chem. Eng.*, 2017, **5**, 4707-4717.

14 Z. H. Yi, Z. Wang, W. W. Nian, T. Wang, H.N. Chen, and Z.Y. Cheng, *ACS Appl. Energy Mater.*, 2021, **4**, 13528-13537.

15 Z. Y. Li, F. H. Liu, H. Li, L. L. Ren, L. J. Dong, C. X. Xiong, Q. Wang, *Ceram. Int.*, 2019, **45**, 8216-8221.

16 Y. C. Xie, J. Wang, Y. Y. Yu, W. R. Jiang, and Z. C. Zhang, *Appl. Surf. Sci.*, 2018, **440**, 1150-1158.

17 D. Kang, G. Y. Wang, Y. H. Huang, P. K. Jiang, and X. Y. Huang, *ACS Appl. Mater.*

Interfaces, 2018, **10**, 4077-4085.

18 S. H. Liu, S. X. Xue, S. M. Xiu, B. Shen, and J.W. Zhai, *Sci. Rep.*, 2016, **6**, 26198.

19 P. H. Hu, S. M. Gao, Y. Y. Zhang, L. Zhang, and C. C. Wang, *Compos. Sci. Technol.*, 2018, **156**, 109-116.

20 P.G. Yang, L. L. Li, H. B. Yuan, F. Wen, P. Zheng, W. Wu, L. Zhang, G. F. Wang, and Z. Xu, *J. Mater. Chem. C*, 2020, **8**, 14910-14918.